

UNCLASSIFIED

---

AD 272 075

*Reproduced  
by the*

ARMED SERVICES TECHNICAL INFORMATION AGENCY  
ARLINGTON HALL STATION  
ARLINGTON 12, VIRGINIA



---

UNCLASSIFIED

**NOTICE:** When government or other drawings, specifications or other data are used for any purpose other than in connection with a definitely related government procurement operation, the U. S. Government thereby incurs no responsibility, nor any obligation whatsoever; and the fact that the Government may have formulated, furnished, or in any way supplied the said drawings, specifications, or other data is not to be regarded by implication or otherwise as in any manner licensing the holder or any other person or corporation, or conveying any rights or permission to manufacture, use or sell any patented invention that may in any way be related thereto.

272 075

CATALOGED BY ASTIA 272075  
AS AD No.

Released to ASTIA for further dissemination with  
out limitations beyond those imposed by security  
regulations.

NAVWEPS REPORT 7796  
NOTS TP 2790  
COPY 75

## RADIOMETRIC TEMPERATURE MEASUREMENTS OF SHORT DURATION EVENTS

XEROX

by  
Earle B. Mayfield  
Research Department

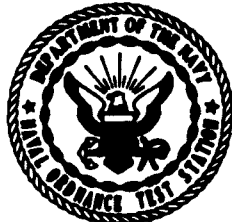
62-2-3

**ABSTRACT.** A four-color spectroscopy using the wavelengths 0.546, 0.577, 0.623, and 0.750 microns was used to determine the surface temperatures of electrically exploded wires and aluminum projectiles of velocity 4,500 m/sec. Several values of initial capacitor energy, pressure, and ambient atmosphere were used with the exploded wires. The projectiles were observed in a normal atmosphere at 710 mm Hg.

The temperatures observed for exploded wires for an initial capacitor energy of 0.8 joule in air at 710 mm Hg were:  $3825 \pm 25^\circ\text{K}$  for aluminum,  $3100 \pm 75^\circ\text{K}$  for copper, and  $3700 \pm 25^\circ\text{K}$  for tungsten. For an aluminum projectile in air at 710 mm Hg at a velocity of 4,500 m/sec, the temperature observed was  $3250 \pm 50^\circ\text{K}$ .

The spectral distribution in all cases was observed to be black body and could be fitted by the Wien radiation law. Calibration was achieved using a tungsten ribbon lamp.

Black-body radiation data from the Planck radiation law are also given using the new value for the second radiation constant,  $C_2 = 14,388 \mu\text{-}^\circ\text{K}$  for temperatures from 2000 to  $4000^\circ\text{K}$  and wavelengths from 0.500 to 0.800 micron.



U. S. NAVAL ORDNANCE TEST STATION

China Lake, California

December 1961

ASTIA

FEB 26 1962

TISIA

A

# U. S. NAVAL ORDNANCE TEST STATION

AN ACTIVITY OF THE BUREAU OF NAVAL WEAPONS

C. BLENNAN, JR., CAPT., USN  
Commander

WM. B. MCLEAN, PH.D.  
Technical Director

## FOREWORD

This report was originally prepared as a thesis in partial fulfillment of the requirements for the degree of Doctor of Philosophy in physics at the University of Utah at Salt Lake City.

The author was a former employee of this Station and since the experimental work and thesis were accomplished here by arrangement with the University of Utah, the thesis is here re-issued as a Station report. The work was partially funded by Bureau of Naval Ordnance Task Assignment NO-803767-73001-01045.

The thesis was reviewed and approved by the thesis supervisory committee: Dr. Gilbert Plain of this Station, and Prof. F. S. Harris, Jr., Dr. Thomas J. Parmley, and Dr. Ray L. Doran of the University of Utah.

CHAS. E. WARING  
Head, Research Department

Released under  
the authority of:  
WM. B. MCLEAN  
Technical Director

NOTS Technical Publication 2790  
NAVWEPS Report 7796

Published by. . . . .Research Department  
Collation. . . . .Cover, 14 leaves, abstract cards  
First printing. . . . .150 numbered copies  
Security classification. . . . .UNCLASSIFIED

## INTRODUCTION

The determination of temperature during time intervals of the order of microseconds and for temperature of the order of thousands of degrees Kelvin is one of the most uncertain and difficult problems to be solved experimentally. Several fundamental difficulties are responsible. Perhaps the most fundamental is the question of energy equilibrium among the degrees of freedom of the system. Unless there is equilibrium, there is no true temperature and any value obtained must be qualified by some statement giving the kind of temperature reported. The difficulty in defining temperature exactly under all conditions of measurement has led to several types of defined temperatures that usually are employed.

True temperature is the value obtained from mechanical measurements such as dimensional changes in the system or measuring device, for example mercury in glass thermometers or bimetallic strips, or from thermocouples and resistance thermometers. Black-body temperature is the temperature of an enclosed cavity in which the spectral energy density is given by the Planck radiation law, Eq. 1. If a small amount of radiation is allowed to escape from the cavity, the temperature can be determined by measuring the spectral intensity as a function of wavelength and using Eq. 8. Color temperature is the temperature of a body whose color matches that of a black body at a known temperature. Radiometrically, color temperature is usually defined from the spectral intensity curve that is fit by Planck distribution of known temperature. Brightness temperature is the temperature determined from measuring the total radiation from a source; if only a narrow wavelength region is used it is called a monochromatic brightness temperature. Optical pyrometers determine the monochromatic brightness temperature of a source and since they have been calibrated against a black body a correction must be made for emissivity or absorption. Translational temperature is obtained from measurements on line broadening in a gas usually at low pressures that is caused by the Doppler effect and hence related to translational velocities. Rotational and vibrational temperatures are determined from measurements of the intensities of rotational and vibrational spectral lines in gaseous spectra. Electronic temperature is determined from measurements of the electronic spectrum of a gas and is based on the intensity distribution of the spectrum.

Another difficulty is that, in general, the electromagnetic radiation distribution from a system cannot be determined from theory so that only for the special cases of black-body and gray-body radiators can a true temperature be obtained from radiometric data.

Using conventional methods requiring physical contact with the system, one is limited to measurements during time intervals of the order of milliseconds or longer and to temperatures less than 2000°K (Ref. 1). Only radiometric observations using photomultiplier tubes offer the speed and range necessary for short duration, high temperature determinations.

Photomultipliers are excellent for radiometric measurements since they are capable of very short time response, and when operated with constant dynode voltage they are linear to changes in radiation (Ref. 2). They are one of the most sensitive radiation detectors available. Present photomultipliers cover the spectral range from about 0.20 micron at the vacuum ultraviolet to about 1.2 micron in the near infrared. Their lower limit on time response is about  $5 \times 10^{-9}$  seconds. When used with a cathode ray oscilloscope, radiometric time-intensity measurements can be made and recorded on cameras with time resolution about  $5 \times 10^{-8}$  seconds.

In 1953 Harris first described a method of the determination of temperatures in detonating explosives that was applied by the Bureau of Mines, Pittsburgh Experimental Station to successfully measure detonation temperatures for a number of explosives (Ref. 3 and 4). This method is based on the assumption that the explosive behaves like a black body for which the spectral energy distribution depends only on the temperature. If one determines the energy distribution, the temperature can be calculated. The work described in this report is based on the method of Harris adapted to fit the different experimental conditions.

### THEORY

The spectral energy density inside an enclosed cavity is given by the Planck radiation law.

$$\rho_{\lambda} = \frac{8\pi ch}{\lambda^5 [\exp(ch/\lambda kT) - 1]} \quad (1)$$

where  $c$  is the velocity of light,  $h$  is the Planck constant, and  $k$  is Boltzmann's constant. The best value of these constants are given by DuMond and Cohen (Ref. 5) as

$$c = 299792.9 \pm 0.8 \text{ km/sec} \quad (2)$$

$$h = 6.6252 \pm 0.0005 \times 10^{-34} \text{ j-sec} \quad (3)$$

$$k = 1.38042 \pm 0.00010 \times 10^{-23} \text{ j/}^{\circ}\text{K} \quad (4)$$

Usually one defines two constants called the first and second radiation constants that are

$$c_1 = 8\pi ch = 4.9919 \pm 0.0004 \times 10^{-24} \text{ j-m} \quad (5)$$

$$c_2 = ch/k = 14,388.4 \pm 0.8 \mu^{\circ}\text{K} \quad (6)$$

Experimentally one is interested in the radiation from a black body rather than the density inside the cavity. It can be shown (Ref. 6) that the relation between monochromatic energy density and monochromatic emissive power or power radiated per unit area per unit wavelength is

$$\psi_{\lambda} = \frac{4e_{\lambda}}{c} \quad (7)$$

Equation 1 then becomes

$$e_{\lambda} = \frac{2\pi c^2 h}{\lambda^5 [\exp(ch/\lambda kT) - 1]} \quad (8)$$

It is customary to write the constant  $2\pi c^2 h$  appearing in Eq. 8 as  $c_1$  despite the confusion with the first radiation constant. Its numerical value is

$$c_1 = 2\pi c^2 h = 3.7413 \times 10^{-16} \text{ watt-m}^2 \quad (9)$$

Within the limits of experimental accuracy, Eq. 8 accurately describes the radiation from a black body for all wavelengths and temperatures. Tables of data calculated from the Planck equation can be found in the American Institution of Physics Handbook (Ref. 7) and elsewhere. However, the results are based on earlier values of the radiation constants and are consequently in error. To bring the radiation data up to date, the Planck equation was programmed on the IBM 704 computer at the Naval Ordnance Test Station (NOTS) and radiation data computed for temperatures between 2000 and 4000°K and wavelengths from 0.500 to 0.800 microns at intervals of 100°K and 0.200 micron. These data are given in Table 1.

For temperatures up to 4000°K and wavelengths up to 1.0 micron, the Wien radiation law is accurate within 3%. Wien's law is

$$e_{\lambda} = \frac{c_1}{\lambda^5 \exp(c_2/\lambda T)} \quad (10)$$

where the constants  $c_1$  and  $c_2$  are given by Eq. 9 and 6 respectively. For most radiometric studies the Wien law is sufficient and because of its simplicity is preferred to the Planck law.

TABLE 1. Black-body Radiation Using the Planck Equation and  $c_1 = 3.941 \times 10^{-16}$  watt  $m^2$  and  $c_2 = 14,388.4 \mu^{\circ}K$

The first six digits give the significant figure and the last digit gives the exponent to the base 10.																						
Wave-length, μ	Temperature, °K											3600	3800	4000								
	2000	2200	2400	2600	2800	3000	3200	3400														
0.500	.675373	0	.249805	1	.742992	1	.136871	2	.411985	2	.817428	2	.148879	3	.252697	3	.404444	3	.616089	3	.899879	3
0.520	.965404	0	.539562	1	.963491	1	.235096	2	.502791	2	.971667	2	.172940	3	.287634	3	.452129	3	.677709	3	.975636	3
0.540	.153440	1	.447989	1	.122910	2	.238721	2	.600336	2	.113223	3	.197267	3	.321983	3	.497741	3	.735029	3	.104406	4
0.560	.179040	1	.575635	1	.152340	2	.347107	2	.703125	2	.129641	3	.221445	3	.355195	3	.540642	3	.787408	3	.110464	4
0.580	.253957	1	.722309	1	.184901	2	.409506	2	.809592	2	.146160	3	.245104	3	.386813	3	.580345	3	.834424	3	.115715	4
0.600	.298592	1	.888105	1	.220273	2	.475092	2	.913173	2	.162537	3	.267925	3	.416475	3	.616508	3	.875849	3	.120158	4
0.620	.373122	1	.107144	2	.258074	2	.543002	2	.102738	3	.173557	3	.289642	3	.443906	3	.648916	3	.911618	3	.123814	4
0.640	.457496	1	.127114	2	.297880	2	.612369	2	.113581	3	.194031	3	.310042	3	.468915	3	.677466	3	.941797	3	.126715	4
0.660	.551443	1	.143546	2	.339243	2	.682354	2	.124220	3	.203801	3	.328965	3	.491386	3	.702147	3	.966556	3	.128904	4
0.680	.654499	1	.171244	2	.381703	2	.752164	2	.134543	3	.222741	3	.346298	3	.511265	3	.723023	3	.986141	3	.130432	4
0.700	.766021	1	.194993	2	.424808	2	.821069	2	.144457	3	.235751	3	.361969	3	.528552	3	.740218	3	.100086	4	.131351	4
0.720	.885226	1	.219567	2	.468123	2	.868417	2	.153332	3	.247761	3	.375946	3	.543293	3	.753900	3	.101104	4	.131718	4
0.740	.101121	2	.244739	2	.511238	2	.953633	2	.162755	3	.253721	3	.388225	3	.555566	3	.764270	3	.101706	4	.131588	4
0.760	.114300	2	.270281	2	.553776	2	.101623	3	.171030	3	.263607	3	.398831	3	.565478	3	.771550	3	.101928	4	.131016	4
0.780	.127956	2	.295976	2	.595396	2	.107580	3	.178671	3	.277411	3	.407809	3	.573154	3	.775974	3	.101806	4	.130053	4
0.800	.141932	2	.321616	2	.635799	2	.113202	3	.185657	3	.285141	3	.415220	3	.578733	3	.777783	3	.101378	4	.128750	4



The derivative of Eq. 8 with respect to wavelength equated to zero yields the equation

$$\lambda_m T = \text{const.} = 2897.9 \mu\text{-}^\circ\text{K} \quad (11)$$

This is the Wien displacement law and gives the relationship between the temperature of a black body and the wavelength for which the monochromatic emissive power is a maximum. The total emissive power of a black body can be determined by integrating Eq. 8 over all wavelengths

$$E = \int_0^\infty e_\lambda d\lambda$$

which yields

$$E = \sigma T^4 \quad (12)$$

This is the Stefan-Boltzmann law and the value of the constant is

$$\sigma = 5.6686 \pm 0.0005 \times 10^{-8} \text{ watts/m}^2 \text{ }^\circ\text{K}^4 \quad (13)$$

Equation 12 gives the total power radiated from unit area of a black body at a temperature, T.

Certain other radiators for which the monochromatic emissive power is a fixed fraction (less than 1) of a black body are called gray-body radiators. The ratio of emissive power of a gray body to that of a black body is called the emissivity or emittance  $\epsilon$  or

$$\epsilon = e_{\lambda g} / e_{\lambda b} \quad (14)$$

For a gray body, Eq. 8 becomes

$$e_\lambda = \frac{\epsilon c_1}{\lambda^5 [\exp(c_2/\lambda T) - 1]} \quad (15)$$

Most solids and liquids are approximately gray bodies with  $\epsilon$  a function of both temperature and wavelength. Data on  $\epsilon(\lambda, T)$  is very inadequate, only for tungsten is there sufficient data (Ref. 8). Theory is not yet available to calculate emissivity for gray-body radiators.

Equations 10, 11, or 12 offer three methods for temperature determinations. The simplest of these is to use Eq. 10 and to make simultaneous radiometric measurements at two or more wavelengths. For two wavelengths  $\lambda_1$  and  $\lambda_2$ , the method is called two color and the ratio of  $e_{\lambda_1}$  to  $e_{\lambda_2}$  is

$$r = e_{\lambda_1}/e_{\lambda_2} = (\lambda_2/\lambda_1)^5 \exp [c_2/T(1/\lambda_2 - 1/\lambda_1)] \quad (16)$$

or taking logarithms to the base  $e$  on both sides of Eq. 16 gives

$$\ln r = \ln (\lambda_2/\lambda_1)^5 + c_2(1/\lambda_2 - 1/\lambda_1) 1/T \quad (17)$$

This can be written as

$$\ln r = A + B/T \quad (18)$$

where  $A = \ln(\lambda_2/\lambda_1)^5$  and  $B = c_2(1/\lambda_2 - 1/\lambda_1)$ . The constants  $A$  and  $B$  are determined by two observations at known temperatures.

By increasing the number of detectors from two to four, one increases the number of calibration curves from one to three since for  $\lambda_1, \lambda_2, \lambda_3$ , and  $\lambda_4$  there are three independent ratios namely:

$$r_1 = e_{\lambda_2}/e_{\lambda_1}, \quad r_2 = e_{\lambda_3}/e_{\lambda_1}, \quad \text{and} \quad r_3 = e_{\lambda_4}/e_{\lambda_1}$$

These may be used as three separate calibration curves using Eq. 18 and two observations at known temperatures or as one curve of  $\ln r$  versus  $\lambda$  using Eq. 17 and as many known temperatures as are necessary.

The use of Eq. 12 for the determination of temperature is theoretically sound but experimentally difficult to employ due to the need of a detector that has a linear response to all wavelengths. In addition no absorbing or scattering media may be present between the detector and the source. Because of these restrictions, Eq. 12 is a less satisfactory method for temperature determination.

Equation 11, however, offers an excellent method especially in the range of temperatures from about 2900°K to about 13,000°K since  $\lambda_m$  occurs in the range of wavelengths for which photomultipliers detect. Using this method, one observes radiation at several wavelengths which occur on both the upper and lower sides of  $\lambda_m$  and determines the value of  $\lambda_m$  from the curve through the data. This method has the advantage that changes in  $\epsilon(\lambda)$  affect the position of  $\lambda_m$  less than they affect  $e_\lambda$  in Eq. 10. Using the two methods simultaneously enables one to obtain, by an iterative process, relative values of  $\epsilon(\lambda, T)$ .

The experiment described in this report employs Eq. 10 and uses four wavelengths to determine temperature.

## INSTRUMENTATION AND CALIBRATION

A four-color spectroscope was employed in this study using the wavelength positions 0.546, 0.577, 0.623, and 0.750 microns. These values were chosen since they occur at easily obtained lines in the mercury and neon spectra and could therefore be quickly and accurately positioned when changes were made. Moreover, still spectra of the phenomena studied indicated that there were no prominent electronic, rotational, or vibrational lines occurring at these wavelength positions (Ref. 9). In addition emission or absorption lines from  $N_2$  or  $O_2$ , though not previously observed, were avoided since these could contribute if excited by the shock wave associated with the phenomena. The wavelength interval observed at each of the positions was 10 angstroms at 0.546 and 0.577 microns, and 40 angstroms at 0.623 and 0.750 microns.

Additional sources of error that could contribute were line broadening in the ballistic shock wave, absorption by  $H_2O$  and  $CO_2$  in the air, and a dissociation continuum due to  $N_2$  and  $O_2$ . Line broadening is due to three causes: (1) Doppler effect, (2) damping of the wave train, and (3) electric and magnetic fields both local and external. Since the second is usually negligible and no external fields were present, only Doppler broadening was significant. The width of a spectral line is given by  $\alpha_D = 7.16 \times 10^{-6} \lambda (T/M)^{1/2}$  where  $M$  is the molecular weight of the emitting atom or molecule. For the OH molecule at a temperature of 2000°K and a wavelength of 3,151 angstroms,  $\alpha_D$  is only 0.0244 angstroms. Doppler broadening becomes important only at extremely high temperatures.

The heat of dissociation of  $N_2$  and  $O_2$  are 7.38 and 5.08 electron volts, respectively. At 3000°K,  $1/2 kT$  is only 0.13 electron volts so that the energy per degree of freedom is at least an order of magnitude too small for dissociation.

The optical path used in this experiment was 1.5 meter and transmission through a normal atmosphere is greater than 98% from 0.3 to 1.0 microns. In the laboratory, the water present was equivalent to 0.0014 cm per m of path so that absorption by water vapor was insignificant.

The spectroscope, which was designed and built by the author, consisted of a field lens that imaged the event on a field slit of 0.25-mm width, a relay lens that collimated the slit on to a front surface, blazed grating of 600 grooves/mm with a first order blaze wavelength of 0.50 micron at a blaze angle of 8 degrees. After diffraction, the field slit was imaged on the slits of the photomultipliers by a 1.5-meter focal-length, front surface, parabolic mirror of  $f/6$ . The plate factor for the instrument was 12 A/mm. The field lens and the relay lens were Kodak Aero Ektar  $f/2.5$ , 7-inch focal-length lenses operated back to back.

The four photomultipliers were mounted in insulated refrigerators similar to the ones used by McDonald and Harris and could be cooled to dry ice temperatures (Ref. 10). However, because of the intensity of the sources it was never necessary to refrigerate. The tubes used were CRC931VA, which are special rugged military type 931, at 0.546 and 0.577 microns and RCA type 7102 at 0.623 and 0.750 microns. Dynode voltages were obtained from a voltage divider network using wire wound resistors and a power supply designed by the author and based on a design of Fellgett (Ref. 11). Regulation was excellent over the range of input values from 105 to 130 volts. A wiring diagram of this instrument is shown in Fig. 1.

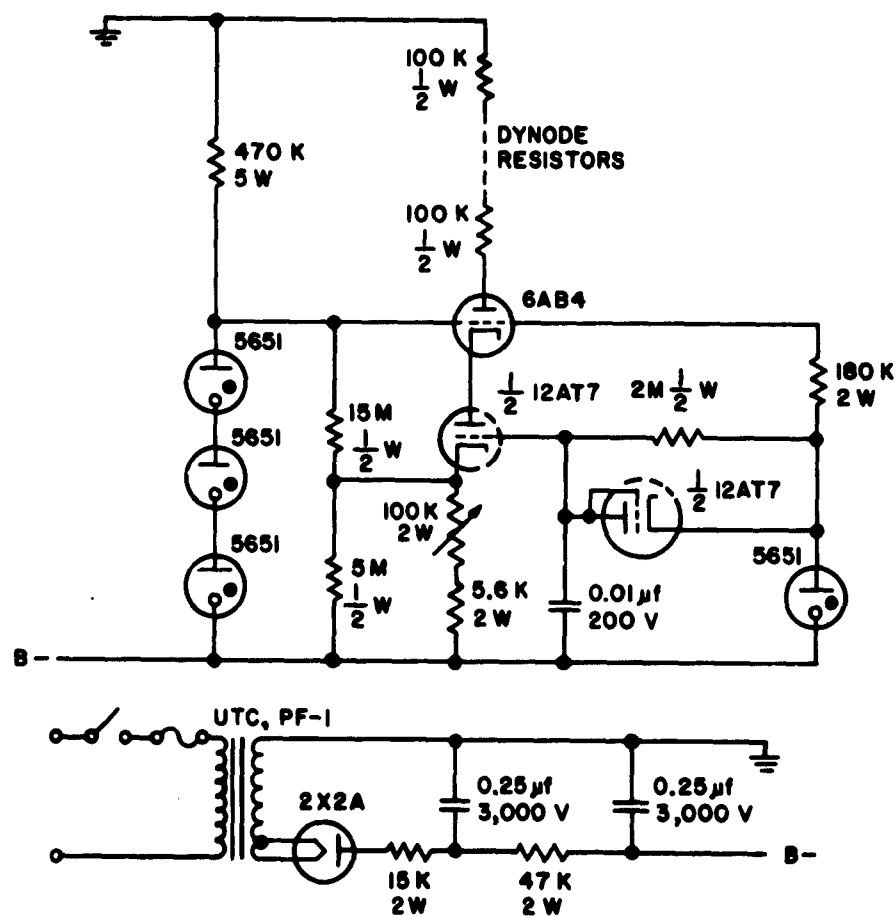


FIG. 1. Wiring Diagram of Regulated Power Supply for Photomultiplier Tubes.

Radiometric data from the photomultipliers were recorded on four Tektronix type 535 oscilloscopes using type 53/54B preamplifiers. These instruments have a band pass of 11 megacycles and a rise time of 0.035  $\mu$ sec. All voltages were developed across deposited carbon 4,000-ohm resistors and coupled through identical 1-meter lengths of RG62/AU cables with a total input shunt capacitance of 45  $\mu$ f. The relaxation time constant for each system was 0.18  $\mu$ sec. Because of this low value, cathode followers were not used. The output signals were photographed with DuMont type 299 oscilloscope cameras on Kodak Royal Pan-type film so that the data could be reduced in a comparator. A schematic diagram of the spectroscope is given in Fig. 2.

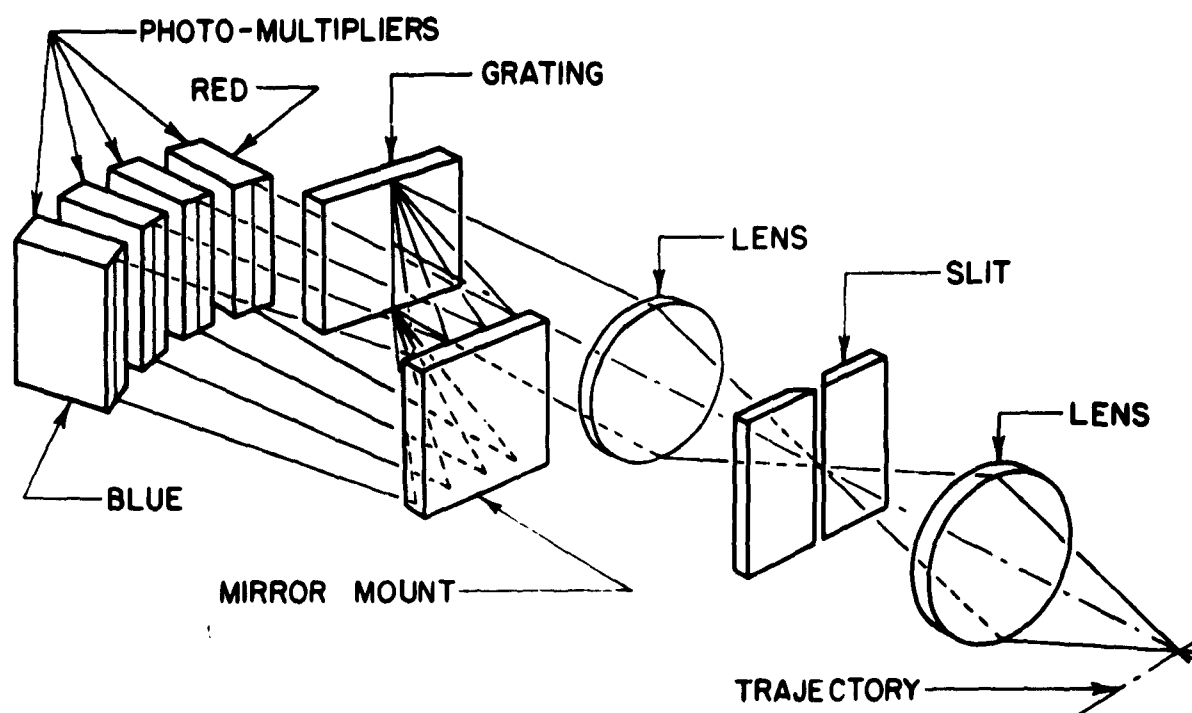


FIG. 2. Schematic of Four-Color Spectroscope

Calibration over the range of temperatures from 1893 to 2743°K was obtained from a tungsten strip filament lamp General Electric type 18AT10/1-6V medium with a type SR8 filament. This lamp has a 2-mm by 18-mm tungsten ribbon and at its rated current of 18 amperes burns at 2670°K. Previous to use it was aged by operating it at 20% overload for 5 hours. Temperature as a function of current was then determined using a calibrated ammeter certified by the Standards Laboratory of NIST and three optical pyrometers calibrated against the Bureau of Standards

secondary standard lamps. Two of the optical pyrometers were Leeds and Northrup types 8622 and 8622-C, the other was a Pyrometer Instrument Company, Pyro Micro-optical-type pyrometer. Lamp temperatures were taken at 1.0-ampere intervals with all three instruments for both increasing and decreasing currents. Over the interval of currents used, the uncertainty in the temperature was about  $\pm 5^\circ\text{K}$ .

To obtain the true temperature of the filament, it is necessary to correct the apparent temperature,  $S$ , obtained with a pyrometer for the emissivity of tungsten at the effective wavelength of the pyrometer filter and for the transmittance of the glass envelope surrounding the filament. The first of these corrections is made using Eq. 10 in the form

$$c_\lambda = \frac{\epsilon(\lambda_e)c_1}{\lambda_e^5 \exp(c_2/\lambda_e T)} \quad (19)$$

where  $\lambda_e$  is the effective wavelength of the filter, and  $\epsilon(\lambda_e)$  is the emissivity of tungsten at  $\lambda_e$ . Information on the effective wavelengths of the pyrometers was obtained from the manufacturers and is given in Table 2. Data for emissivity was taken from Ref. 8.

TABLE 2: Effective Wavelengths of Optical Pyrometer Filters at Various Temperatures

Leeds and Northrup		Pyro Micro-Optical Pyrometer	
Wavelength, $\mu$	Temperature, $^\circ\text{K}$	Wavelength, $\mu$	Temperature, $^\circ\text{K}$
0.656	1144 <sup>a</sup>	0.6553	1273
0.656	1419 <sup>b</sup>	0.6533	1473
0.656	1881 <sup>c</sup>	0.6516	1673
0.655	1255 <sup>a</sup>	0.6499	1873
0.655	1593 <sup>b</sup>	0.6484	2073
0.655	2201 <sup>c</sup>	0.6470	2273
0.654	1366 <sup>a</sup>	0.6458	2473
0.654	1776 <sup>b</sup>	0.6446	2673
0.654	2567 <sup>c</sup>	0.6435	2873
0.653	1477 <sup>a</sup>	0.6426	3073
0.653	1969 <sup>b</sup>	0.6417	3273
0.653	3000 <sup>c</sup>	0.6408	3473

<sup>a</sup> Low range.

<sup>b</sup> High range.

<sup>c</sup> Extra high range.

Substituting the observed temperature,  $S$ , in Eq. 10 and equating to Eq. 19 yields

$$\frac{1}{T_1} - \frac{1}{S} = \frac{\lambda_e \ln \epsilon}{c_2} \quad (20)$$

where  $T_1$  is the temperature of the filament corrected for emissivity. To correct for transmittance Eq. 10 becomes

$$\epsilon_\lambda = \frac{Tr c_1}{\lambda_e^5 \exp(c_2/\lambda_e T)} \quad (21)$$

where  $Tr$  is the transmittance of the glass envelope. This is determined by using a second lamp operated at temperature  $T_2$  as determined by the pyrometer. The standard lamp is then placed in the optical path between the pyrometer and lamp number two and a second temperature  $T_3$  determined by observing the filament through both walls of the standard lamp. Substituting  $T_2$  into Eq. 10 and equating to Eq. 21 yields

$$\frac{1}{T_2} - \frac{1}{T_3} = \frac{\lambda_e \ln Tr^2}{c_2} \quad (22)$$

The transmittance of the glass envelope determined from Eq. 22 is then used to obtain the true temperature,  $T$ , of the filament or

$$\frac{1}{T} = \frac{1}{S} + \frac{\lambda_e}{c_2} (\ln \epsilon + \ln Tr) \quad (23)$$

The lamp used in this experiment had a transmittance of 0.929. Corrections to be made to temperatures observed with an optical pyrometer from 2000 to 4000°K are given in Table 3. These are of course monochromatic brightness temperatures.

#### EXPERIMENTAL

Two phenomena were studied that the author's previous experience had indicated were of interest (Ref. 12 and 13). These were the surface temperatures of exploding wires and the stagnation surface temperatures of hypervelocity projectiles. Extensive literature exists on the exploding wire phenomenon that is presently attracting renewed interest and investigation (Ref. 14-16). The problem of surface temperatures of very high velocity projectiles (above about 1,500 m/sec) is only just beginning to be investigated and outside of classified military documents little literature exists (Ref. 17 and 18). There is a considerable effort being applied to this problem both experimentally and theoretically.

TABLE 3. Temperature Corrections for Transmittance and Emittance

Observed temperature, °K	Temperature correction, °K	True temperature, °K
2000	175	2175
2200	218	2418
2400	265	2665
2600	317	2917
2800	374	3174
3000	436	3436
3200	504	3704
3400	581	3981
3600	661	4261
3800	727	4527
4000	845	4845

The exploding wire phenomenon occurs when a capacitor charged to a high voltage is discharged through a fine metal wire. The accepted model of the process occurring in the wire is that current through the wire increases to a very large value, of the order of  $10^5$  amperes, which heats it to a temperature sufficient to vaporize it (Ref. 19). It expands adiabatically while reducing electrical conduction to a small fraction of the initial maximum and remains in this nonconducting or dwell condition until the metal has expanded sufficiently to acquire gaseous characteristics. Internal collisions then create enough ion pairs to cause avalanching and a second conduction period occurs usually much longer than the first. The time of the process varies from a few microseconds to as long as 10  $\mu$ sec for the first maximum and from about 10 to 100  $\mu$ sec for the second maximum depending on circuit parameters, type wire, and energy stored in the capacitor, as well as initial voltage on the capacitor. Figure 3 is a typical radiant intensity versus time trace for an exploding wire showing the first maximum at about 3  $\mu$ sec and the secondary maximum occurring at about 70  $\mu$ sec. In this case the wire was 0.001-inch tungsten and the capacitor 0.1  $\mu$ f charged to 5,000 d.c. or 1.2 joule. The dwell time that occurs at about 10  $\mu$ sec is of very short duration. Copper, however, behaves significantly different as can be seen in Fig. 4. The first maximum occurs at about 3  $\mu$ sec, the dwell at about 8  $\mu$ sec, and the secondary pulse occurs with a very short rise time at about 60  $\mu$ sec. The secondary pulse is of very short duration and is quite similar to the first maximum except for its much greater amplitude due to its greater surface area. In the case of aluminum, the secondary maximum is negligible or absent as can be seen in Fig. 5, which shows the first maximum at about 2.8  $\mu$ sec and no secondary maximum. The lack of a secondary maximum for aluminum is unusual since its ionization potential of 5.984 electron volts



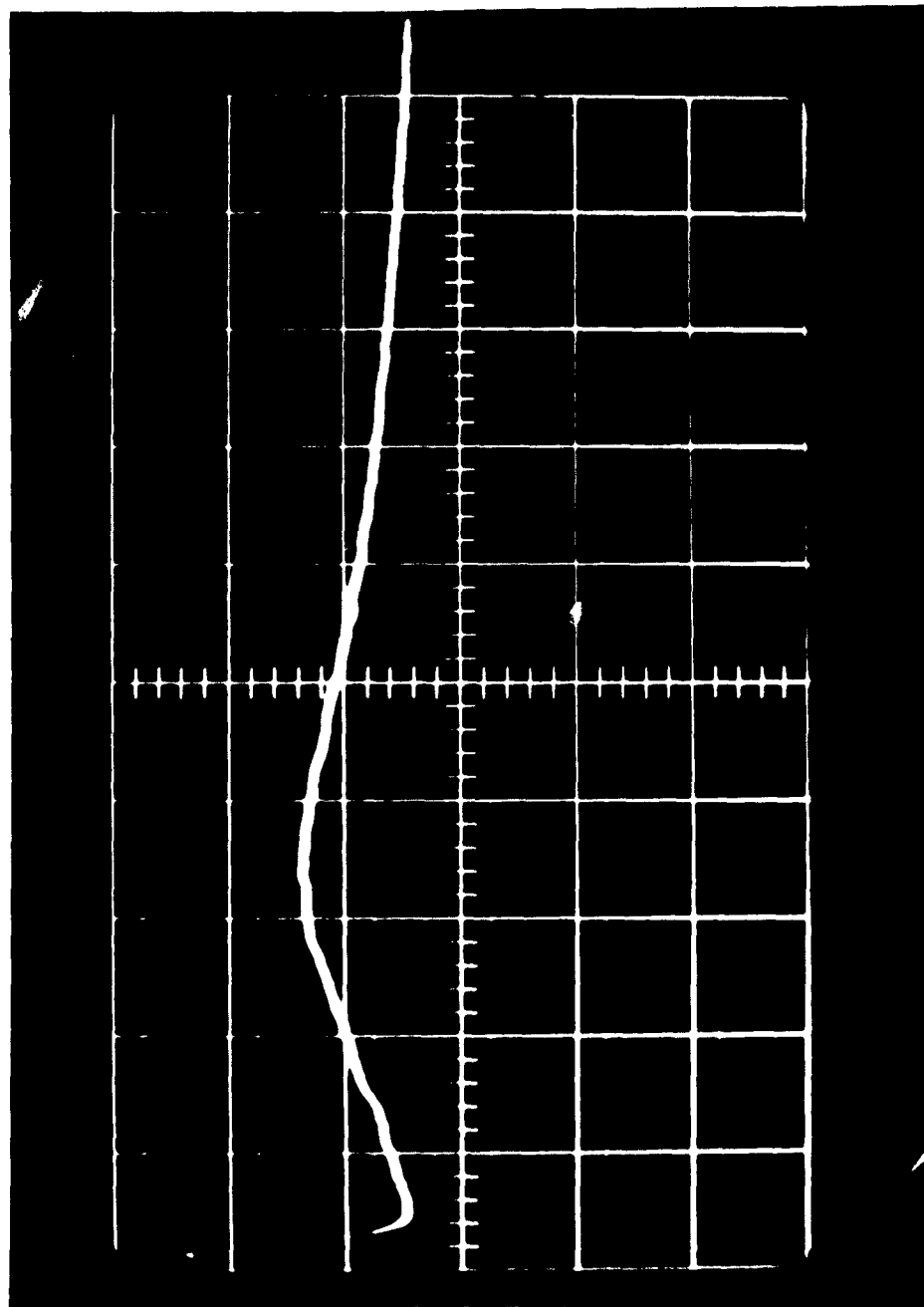


FIG. 3. Time-Intensity Curve for 0.001-Inch Tungsten Wire Exploded by 5,000 Volts d.c. on 0.1-Microfarad Capacitor. The time scale is 20  $\mu\text{sec/cm}$ .

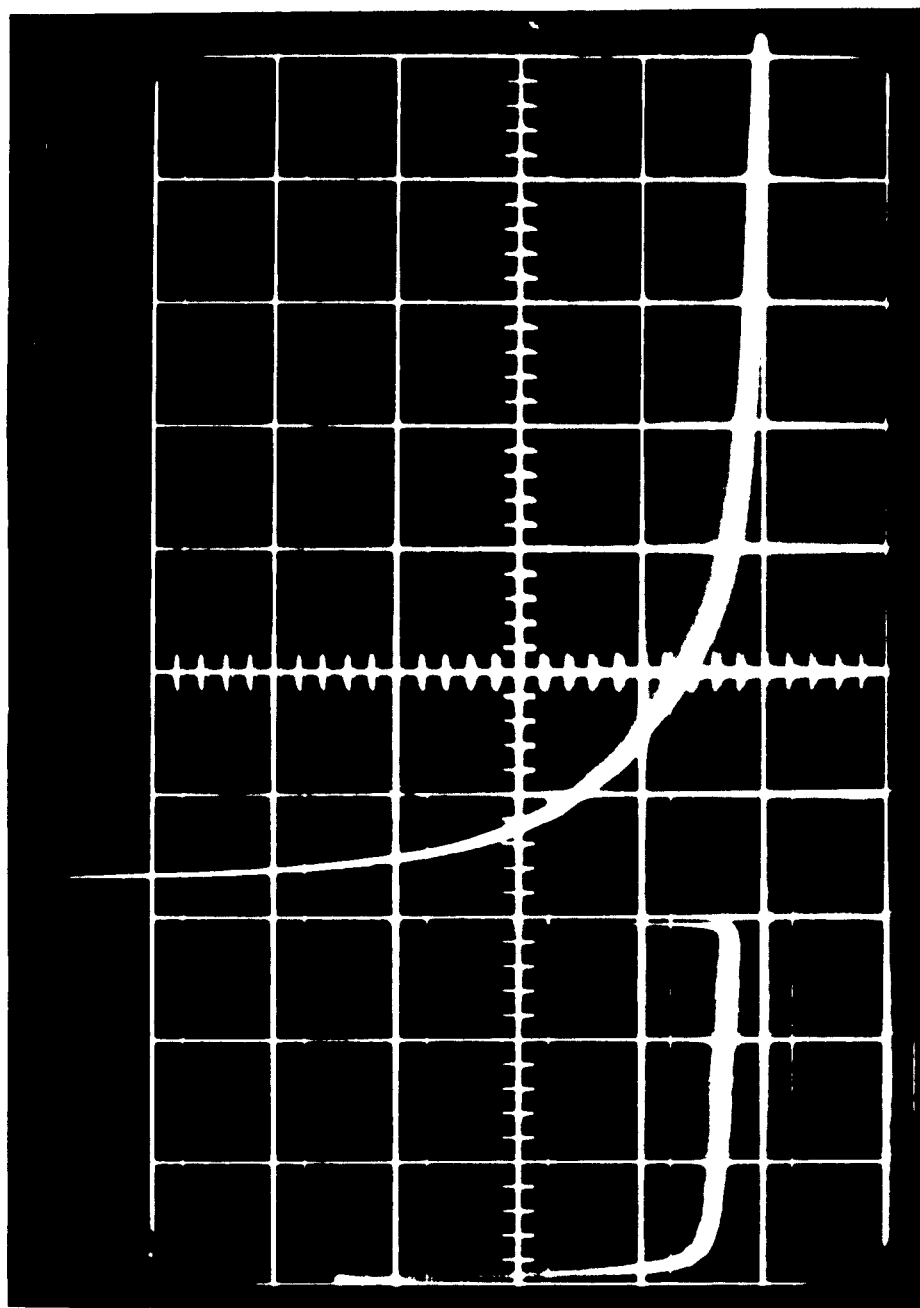


FIG. 4. Time-Intensity Curve for 0.001-Inch Copper Wire Exploded by 4,000 Volts d.c. on 0.1-Microfarad Capacitor. The time scale is 20  $\mu$ sec/cm.

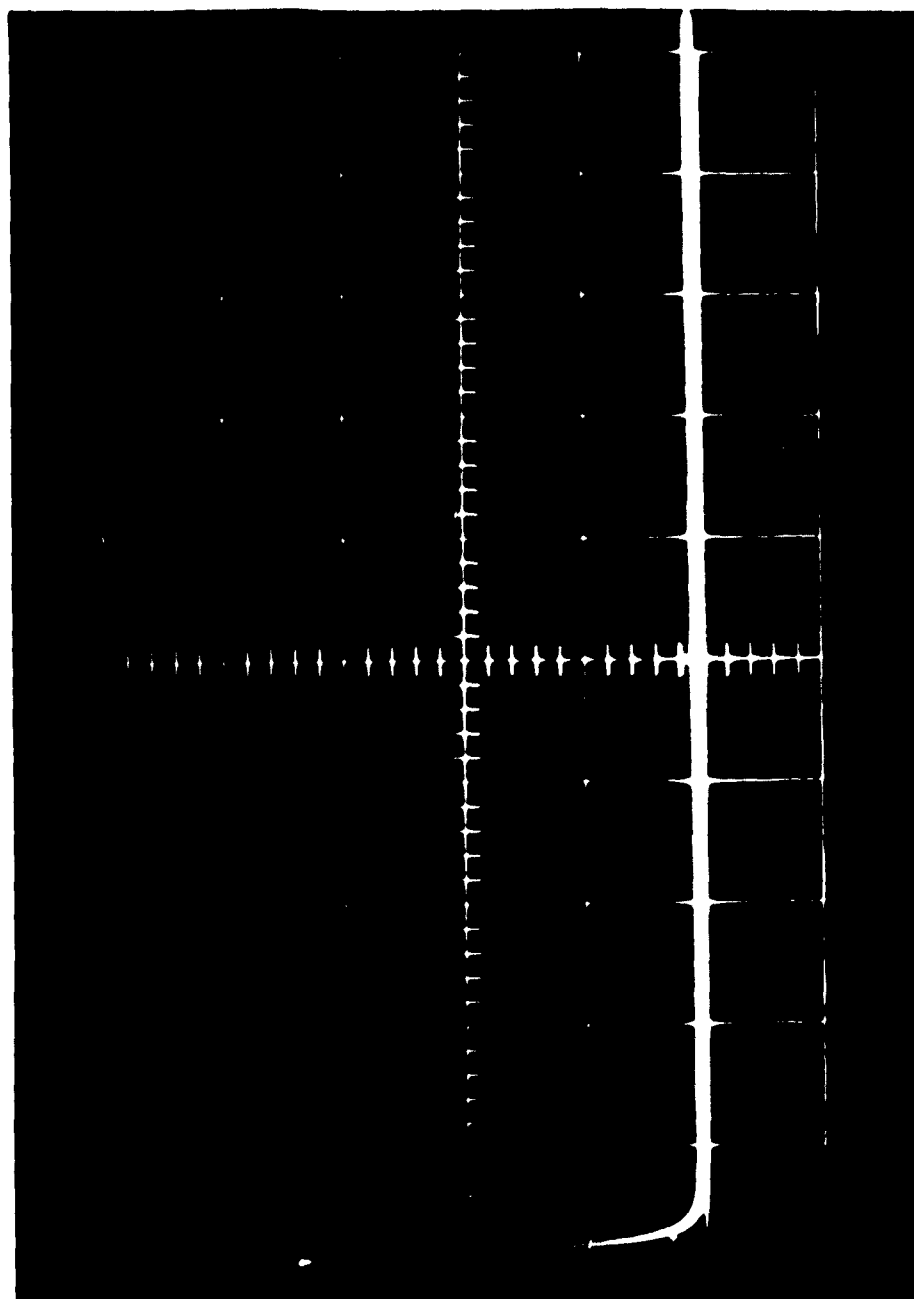


FIG. 5. Time-Intensity Curve for 0.001-Inch Aluminum Wire Exploded by 5,000 Volts d.c. on 0.1 Microfarad Capacitor. The time scale is 20  $\mu$ sec/cm.

is lower than either copper with 7.723 or tungsten with 7.98 electron volts. Insufficient data exists at the present time to explain this behavior.

The equivalent circuit of the exploding wire phenomenon is a series resistance, inductance, capacitance (RLC) circuit. An excellent discussion of the transient behavior of such a circuit can be found in Ref. 20. The second order linear differential equation to be solved is

$$L \frac{d^2 Q}{dt^2} + R \frac{dQ}{dt} + \frac{1}{C} Q = 0 \quad (24)$$

where Q is the charge on the capacitor. Since R is less than 1 ohm, the circuit is underdamped and hence oscillatory. The pseudo frequency is customarily referred to as the ringing frequency.

$$Q = e^{-(R/2L)t} \left[ A \cos \left( \frac{1}{LC} - \frac{R^2}{4L^2} \right)^{1/2} t + B \sin \left( \frac{1}{LC} - \frac{R^2}{4L^2} \right)^{1/2} t \right] \quad (25)$$

from which the ringing frequency is

$$f_r = \frac{1}{2\pi} \left( \frac{1}{LC} - \frac{R^2}{4L^2} \right)^{1/2} \quad (26)$$

Equation 26 is usually used to determine the circuit inductance, since at the frequencies involved in exploding wire phenomenon the impedance is largely inductive. The resistance is usually small so that Eq. 26 reduces to

$$f_r = \frac{1}{2\pi} \left( \frac{1}{LC} \right)^{1/2} \quad (27)$$

that can be solved for L from the experimentally determined ringing frequency. In the apparatus used in this experiment C was  $10^{-7}$  farad and  $f_r$  was  $3.93 \times 10^5$  cycles/sec, this gives  $1.6 \times 10^{-6}$  henrys for the circuit inductance. For an inductance-capacitance circuit the total impedance Z is given by

$$Z = \left( \frac{L}{C} \right)^{1/2} \quad (28)$$

and from the values of L and C, Z is 4 ohms and for an initial capacitor voltage of 5,000 volts the current is 1,250 amperes. As a matter of interest, the inductance of the exploding wire circuit measured with an impedance bridge was  $1.6 \times 10^{-6}$  henrys.

An approximate temperature can be calculated for an exploding wire if certain simplifying approximations are made. First, that the wire terminates the discharge cable in its characteristic impedance so that the power transfer is a maximum, and second, that switch losses and radiation losses are small and can be neglected. The energy stored in the capacitor is then expended heating the wire to its melting temperature, supplying the heat of fusion,  $\Delta H_F$ , heating it to the boiling temperature,

supplying the heat of vaporization, and finally heating the gas (which one assumes monatomic) to the observed temperature. Since the wire does not expand appreciably during the rise to the first maximum, work done on the environment can be neglected. Heat data for the wires used are given in Table 4 for an initial capacitor energy of 1.0 joule; the calculated results for aluminum, copper, and tungsten wire 0.025 mm in diameter and 27 mm in length are given in Table 5. The calculations of Table 5 show that aluminum should have a final temperature of about 10,000°K; tungsten should just be at its boiling temperature of about 6000°K having insufficient energy to vaporize all of the material present, and that copper should be about 4000°K.

TABLE 4. Heats of Fusion and Vaporization, Melting and Boiling Temperatures for Aluminum, Copper, and Tungsten

Wire material	Melting temp., °K	Boiling temp., °K	Heat of fusion, kcal/mole	Heat of vaporization, kcal/mole	Average heat capacity at constant vol., cal/mole
Aluminum	933	2600	2.6	67.9	7.00
Copper	1356	2855	3.11	72.8	7.50
Tungsten	3653	5900	8.4	176	7.26

TABLE 5. Calculated Temperatures of Aluminum, Copper, and Tungsten Wires 0.025 mm Diameter and 27 mm Long for 1.0-Joule Energy Input

Wire material	Energy to melt, joule	Heat of fusion, joule	Energy to boil, joule	Heat of vaporization, joule	Energy to heat gas, joule	Final temp., °K
Aluminum	0.025	0.013	0.063	0.368	0.531	10000
Copper	0.063	0.025	0.088	0.577	0.247	4000
Tungsten	0.142	0.050	0.096	1.028	.....	5900

The experimentally observed temperatures were significantly lower than those values reflecting the error due to disregarding such losses as radiation that increase according to the Stefan-Boltzmann law proportional to  $T^4$  and switching losses. Radiation losses, however, do not account for the major loss since for the wire used in this experiment the surface area is  $2.12 \times 10^{-4} \text{ m}^2$  and from Eq. 13 the power radiated even at  $10,000^\circ\text{K}$ , assuming black-body conditions, is only  $1.2 \times 10^4$  watts, or during the  $3 \mu\text{sec}$  of buildup is only 0.036 joule. This value is inadequate to explain the discrepancy. Losses in impedance mismatch and switching that cannot be easily determined can account for the difference.

Several values of input energy were used and various gases as well as reduced air pressures were used to determine the influence of these parameters on the observed temperature. The use of carbon dioxide and helium did not reduce the experimental scatter in the data, in fact the results were negative and no gray-body curve could be fit to the data. Reducing the pressure caused a decrease in the temperature to 500 mm Hg but below this pressure arcing occurred so that the wire could not be exploded. In addition the error increased significantly. The excellence of the data in normal air at one atmosphere and the errors introduced by either pressure reduction or other gases indicate that atmospheric air is preferred. Table 6 gives all the data for exploding wires and the average values for each change of variable. Table 7 gives average temperature observed experimentally and the calculated temperatures for the different energies. It is seen that the predicted temperatures are significantly higher than the experimentally observed temperatures but that the predicted order among the three metals used is correct.

The second phenomenon studied is the stagnation surface temperature of an ultraspeed projectile that is raised to a high temperature by aerodynamic heating. Aluminum projectiles were chosen because of their high strength to density ratio and because of the author's experience in studying the luminous wake of these projectiles (Ref. 12, 21 and 22). A physical description of these projectiles and methods for acceleration by means of high explosives has been given by Van Valkenburg and Hendricks (Ref 23). Velocities obtained for aluminum projectiles with this method are about 4,500 m/sec.

Several difficulties arise in connection with the projectiles. Their trajectories are randomly distributed about the intended flight axis so that only about 20% of them pass through the field of the spectroscopy. One other problem is that the shock waves from the explosive charge will damage the equipment unless heavy shielding is present to protect it.

Projectile velocity was measured using a General Radio type 651 AH high speed streak camera. Film velocity was determined by means of a General Radio Strobotac calibrated by the Standards Laboratory of NTS. A still photograph was taken of each projectile to establish the

TABLE 6. Complete Output Signal Data for 0.001-Inch Aluminum, Copper, and Tungsten Wires Electrically Exploded for Several Values of Capacitor Energy and Ambient Air Pressure

The output signal was developed across identical 4,000-ohm resistors.

Capacitor energy, joule	Ambient pressure, mm Hg	Output signal in volts at each of the 4 wavelengths			
		0.546μ	0.577μ	0.623μ	0.750μ
A. Aluminum Wire					
0.8	710	0.685	0.464	0.515	0.210
0.8	710	1.220	0.820	0.650	0.340
0.8	710	2.161	1.462	1.440	0.680
0.8	710	0.735	0.525	0.226	0.200
0.8	710	1.593	1.011	0.495	0.535
0.8	710	1.060	0.680	0.306	0.186
0.8	710	1.850	1.290	1.202	0.620
0.8	710	1.831	1.401	0.730	0.525
0.8	710	0.640	0.470	0.191	0.197
0.8	710	0.665	0.499	0.550	0.222
0.8	710	0.770	0.560	0.392	0.202
0.8	507	1.903	1.320	0.722	0.463
0.8	507	1.155	1.042	0.608	0.417
0.8	507	2.960	2.030	1.441	1.002
1.0	305	1.581	1.060	0.615	0.496
1.0	305	2.802	1.911	0.955	0.706
1.0	305	2.511	1.732	1.262	0.686
1.0	305	1.260	0.856	1.050	0.412
1.0	305	1.951	1.321	1.170	0.620
1.8	303	4.882	4.353	2.091	1.602
1.8	303	5.242	4.663	1.951	1.620
1.8	303	2.122	1.470	0.870	0.701
B. Tungsten Wire					
0.8	710	2.640	1.761	1.052	0.683
0.8	710	2.589	2.028	1.160	0.755
0.8	710	1.258	1.041	0.462	0.355
0.8	710	2.382	1.593	1.009	0.757
0.8	710	2.778	1.871	1.101	0.841
0.8	710	3.637	2.353	1.109	0.876
0.8	710	2.757	2.020	1.593	1.211
0.8	710	2.720	2.103	1.289	0.897
0.8	710	1.600	1.127	0.732	0.654
0.8	710	2.484	1.693	1.089	0.757
0.8	710	2.868	1.909	1.233	0.854

TABLE 6. (Continued)

Capacitor energy, joule	Ambient pressure, mm Hg	Output signal in volts at each of the 4 wavelengths			
		0.546 $\mu$	0.577 $\mu$	0.623 $\mu$	0.750 $\mu$
C. Copper (Insulated) Wire					
0.8	710	2.292	0.781	0.374	0.320
0.8	710	1.179	0.555	0.316	0.297
0.8	710	0.770	0.548	0.137	0.170
0.8	710	1.533	0.608	0.214	0.228
0.8	710	1.318	0.626	0.248	0.270
0.8	710	1.032	0.650	0.216	0.244
0.8	710	0.980	0.694	0.213	0.223
0.8	710	1.355	0.836	0.339	0.298
0.8	710	0.845	0.724	0.105	0.374
D. Copper (Bare) Wire					
0.8	710	0.714	0.605	0.289	0.320
0.8	710	1.010	0.635	0.331	0.335
0.8	710	0.782	0.538	0.221	0.232
0.8	710	0.985	0.477	0.186	0.185
0.8	710	0.565	0.580	0.299	0.305
1.5	710	1.011	0.950	0.461	0.490
1.5	710	1.047	0.941	0.417	0.468
1.5	710	0.973	0.892	0.495	0.517
1.5	710	1.034	1.008	0.461	0.493

trajectory and whether the projectile broke up or tumbled. To ensure that the spectroscope observed the surface of the projectile, the optical axis was inclined 17 degrees off the normal to the projectile axis so that the field slit allowed only a section of the surface to be observed by the photomultipliers. Unless this latter precaution is taken, the spectroscope will give an integrated temperature of the entire surface, or what is more usual, observe only the wake that is mostly  $AlO^{11}$ . A typical radiometric record of an aluminum projectile at a velocity of 4,500 m/sec in normal air at 710-mm-Hg pressure, 1.5 meters after launching is given in Fig. 6. The sweep time of the oscilloscope was 2  $\mu$ sec/cm and the maximum intensity occurs at about 1.8  $\mu$ sec after entering the field of view of the spectroscope. The two traces appearing near the horizontal center line of the graticule are due to the wake that occurs about 100  $\mu$ sec after the passage of the projectile (Ref. 24).

To determine the stagnation (or total) temperature of a blunt projectile normal to the flow of a gas of molar heat capacity,  $C_p$  joules/mole-°K, one assumes that the kinetic energy of the moving gas is



TABLE 7. Computed and Average Observed Temperatures of 0.001-Inch Aluminum, Copper, and Tungsten Wires Electrically Exploded for Several Values of Capacitor Energy and Ambient Air Pressure

Wire material	Capacitor energy, joule	Ambient pressure, mm Hg	Computed temp., °K	Observed temp. for black body, °K	Observed temp. for two color, °K
Aluminum	0.8	710	73 00	3825 ± 25	3725 ± 125
Aluminum	0.8	500	73 00	3700 ± 25	3573 ± 175
Aluminum	1.0	300	100 00	3600 <sup>a</sup>	3450 ± 100
Aluminum	1.8	300	210 00	no fit	3360 ± 150
Tungsten	0.8	710	59 00	3700 ± 25	3550 ± 125
Copper (insulated)	0.8	710	31 00	no fit	3470 ± 400
Copper (bare)	0.8	710	31 00	3100 ± 75	2960 ± 100
Copper (bare)	1.50	710	62 00	2770 ± 50	2700 ± 150

<sup>a</sup> Approximate.

completely expended in heating the gas as it accelerates to zero velocity at the surface of the projectile. Assuming no other losses such as radiation or heat transfer, the heat energy per unit mass,  $C_p T_0$ , and the kinetic energy per unit mass,  $1/2 V^2$ , must be constant or

$$C_p T_0 + 1/2 V^2 = \text{constant} \quad (29)$$

where  $T_0$  is the initial temperature of the gas and  $V$  is the velocity of the gas (in this case the projectile velocity). When  $V$  is zero, the temperature is the stagnation temperature,  $T_s$ . The constant is therefore  $C_p T_s$  and

$$C_p T_0 + 1/2 V^2 = C_p T_s \quad (30)$$

from which

$$T_s/T_0 = 1 + V^2/2C_p T_0 \quad (31)$$

Assuming ideal gas behavior,  $R = C_p - C_v$ . The Mach number is  $M = V/c$  where  $c$  is the local sound velocity in the gas and is also given by  $c = \sqrt{\gamma R T_0}$  (Ref. 7, sec. 3, p. 32). Equation 24 then simplifies to

$$T_s = T_0 [1 + (\gamma - 1)/2M^2] \quad (32)$$

where  $\gamma = C_p/C_v$ . Under the conditions of this experiment,  $c = 347$  m/sec,  $V = 4,500$  m/sec,  $\gamma = 1.40$ ,  $M = 13.0$ , and  $T_0 = 300^\circ\text{K}$ . Using these values in Eq. 30 gives a stagnation temperature of  $T_s = 10,000^\circ\text{K}$ .

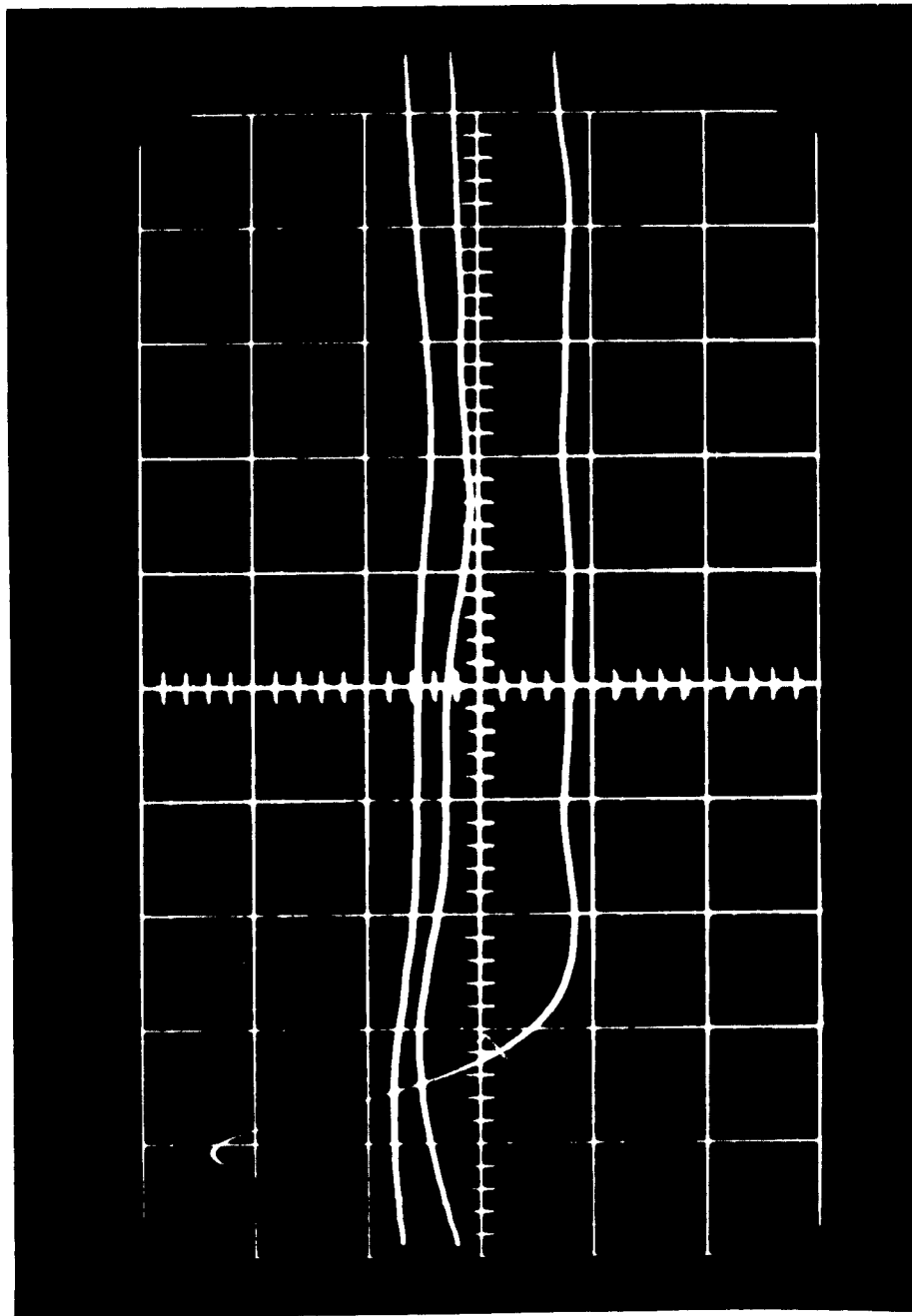


FIG. 6. Time-Intensity Curve for a Blunt Aluminum Projectile at a Velocity of 4,500 ft/sec in Air at 710 mm Hg. The time scale is 2  $\mu$ sec/cm. The retrace lines near the center are due to the wake.

The experimentally observed temperature of the projectile had an average value of  $3250 \pm 50^\circ\text{K}$  based on a gray-body curve of best fit through the data. The two-color method gave an average value of  $3015 \pm 200^\circ\text{K}$ . The data was deficient in the yellow at 0.577 micron by about 6% but gave a good gray-body fit at the other points. Because of the yellow deficiency, the two-color ratio method gave a greater error than the gray-body method. All data for the aluminum projectiles is given in Table 8.

TABLE 8. Complete Output Signal Data for 1/2-Inch  
75 ST Aluminum Projectiles in Normal Air at 1  
Atmosphere for Velocity 4,500 Meter/Second

The output signal was developed across identical  
4,000-ohm resistors.

Ambient Pressure, mm Hg	Air Temp., °K	Output signal in volts at each of the 4 wavelengths			
		0.546 $\mu$	0.577 $\mu$	0.623 $\mu$	0.750 $\mu$
705.5	295.7	2.73	1.67	0.968	0.850
708.9	296.3	0.601	----	0.565	0.464
708.5	299.8	2.19	1.37	0.682	0.650
708.5	299.8	1.17	0.600	0.534	0.464
706.9	296.1	1.60	0.855	0.730	0.640
706.9	296.1	0.960	0.501	0.442	0.384
707.0	296.1	1.73	0.715	0.378	0.334
708.0	296.6	2.29	1.75	0.514	0.518
710.2	296.9	0.800	0.464	0.328	0.242

The temperature obtained in this study can be used to give an estimate of the equilibrium distribution of heat between projectile and air which is one of the problems that heat transfer studies must answer. Aerodynamic studies by Allen, Rinehart, and White (Ref. 25) of explosive driven projectiles showed that the projectile obeys the following drag law

$$V = V_0 \exp(-\alpha s) \quad (33)$$

where  $V_0$  is the velocity when  $s = 0$ . For aluminum the value of  $\alpha$  is  $0.050 \text{ m}^{-1}$ . The acceleration is then given by

$$a = dv/dt = -\alpha V_0 \exp(-\alpha s) ds/dt \quad (34)$$

or using Eq. 31

$$a = -\alpha V^2 \quad (35)$$

For a velocity of 4,500 m/sec, the acceleration is  $2 \times 10^5$  m/sec<sup>2</sup> and the loss of kinetic energy is  $6 \times 10^5$  watts. Loss of energy due to ablation is negligible since White has shown that it is of the order of micrograms per meter of path (Ref. 26). The loss due to radiation is, assuming a value of 0.4 for the total emissivity of aluminum, about 275 watts and the ratio of heat absorbed by the air to heat absorbed by the projectile is 2,200.

### DISCUSSION

The results of the preceding section show that for the two phenomena studied the spectral distribution could be fit very accurately by the radiation laws and that the uncertainty in the temperature was a few percent. Except for the case of insulated copper wire and aluminum wire in a partial vacuum where the observed distribution departed from black-body characteristics, both methods of fitting the data gave agreement within the limits of uncertainty.

One of the significant facts is that the temperature decreased with increasing capacitor voltage even though the initial energy increased. The assumptions on which the calculations of Table 7 were based were that only the initial energy of the system would change and that the first current peak would remain constant. The explanation of the observed behavior is that under the conditions of the experiment, a part of the initial energy goes into the second or gaseous conduction stage whereas the calculations were based on the assumption that all of the energy would go into the first stage. Photographs obtained by Zernow on the behavior of an exploding wire during the initial stages of heating show that the pinch effect strongly influences the wire (Ref. 16). Typically, saucer instabilities occur that cause separation of the wire into discrete bubbles that burst to form saucer shaped disks. Usually there are several disks (as many as 10 or 20) formed that effectively interrupt the current flow. With increasing initial currents, the time required for the onset of instability is reduced and current conduction stopped with less of the capacitor energy expended. Two results should be observed because of this: (1) the temperature of the first pulse should be lower, and (2) the second pulse should contain more of the energy and occur earlier in time since the electric field strength is greater in this case. Both of these effects were observed in this experiment. For example with copper wire at 4,000 volts the second pulse occurs at 60  $\mu$ sec but at 5,500 volts it occurs at 8  $\mu$ sec. The amplitude of the second pulse at the higher voltage was much greater and of longer duration.

The heat ratio factor determined for projectiles is limited by the fact that the body does not have a large heat capacity and hence represents radiative equilibrium imposed by the stagnation temperature that

in turn depends on the stagnation pressure. Allen and others have shown that for projectiles of the type used in this study the average pressure of the surface of the projectile is about 150 atmospheres (Ref. 25). Since the projectile was boiling at its observed temperature of 3250°K, the average pressure on its surface is its vapor pressure also.

The results of this study represent only the beginning of the work which can be done using the methods described in it. Its use as a research tool to a number of similar problems is certain to yield valuable information on problems of equilibrium and temperature.

### CONCLUSIONS

This study has shown that the temperature of transient phenomena such as an electrically exploded wire or an explosively driven projectile can be determined during microsecond intervals of time. The spectral energy distribution from the surface of the event agrees closely with the predictions of either the Planck or Wien radiation laws and yields a temperature with an uncertainty of a few percent. The applications to exploding wires and hypervelocity projectiles have shown that surface temperatures of the order of several thousand degrees Kelvin exist, in general agreement with theory.

The importance of this method lies in the fact that it gives a powerful new method for obtaining data for developing adequate theories. This is especially true in the area of hypersonic aerodynamics where data on stagnation temperatures at the velocities studied here are not available.

Its application to the exploding wire phenomenon will yield relative spectral emissivity data on metals at temperatures even beyond the critical temperature. By comparison with tungsten, for which good emissivity data exist, an absolute calibration can be made and extensive  $\epsilon(\lambda, T)$  data obtained.

# REFERENCES

1. Hoge, Harold J. "Temperature Measurement in Engineering," in Temperature, Its Measurement and Control in Science and Industry, Vol. II. New York, Reinhold, 1955. Pp. 287-325.
2. Radio Corporation of America. "Photosensitive Devices," in RCA Tube Handbook, HB-3. Harrison, New Jersey, RCA, 1957.
3. University of Utah, Explosives Research Group. The Measurement of Temperature in Explosives, by F. S. Harris, Jr. Salt Lake City, Utah, Univ. of Utah, August 1953. (Technical Memorandum.)
4. Gibson, F. C., M. L. Bowser, C. R. Summers, F. H. Scott, and C. M. Mason, J APPL PHYS, 29, 628 (1958).
5. DuMond, J. W. M., and E. R. Cohen. REV MOD PHYS, 25, 691 (1953).
6. Richtmyer, F. K., and E. H. Kennard. Introduction to Modern Physics. New York, McGraw-Hill, 1947. Pp. 178-183.
7. American Institute of Physics. American Institute of Physics Handbook. New York, McGraw-Hill, 1957.
8. DeVos, J. C. PHYSICA XX, 690 (1954).
9. White, W. C., J. S. Rinehart, and W. A. Allen. J APPL PHYS, 24, 198 (1952).
10. McDonald, K. L., and F. S. Harris, Jr. OPT SOC AM, J, 42, 321 (1952).
11. Fellgett, P. J. J SCI INSTR, 31, 217 (1954).
12. Allen, W. A., and E. B. Mayfield. J APPL PHYS, 24, 131 (1953).
13. Allen, W. A., C. D. Hendricks, Jr., E. B. Mayfield, and F. N. Miller. REV SCI INSTR, 24, 1068 (1953).
14. Air Force Cambridge Research Center. A Bibliography of the Electrically Exploded Wire Phenomenon, by W. G. Chace. Boston, Mass., AFRCRC, 1956. (Technical Memorandum GRD-TM-57-5.)
15. Conn, W. M. Z ANGEW PHYS, 7, 539 (1955).

16. Chace, William G., and Howard K. Moore, eds. Exploding Wires. New York, Plenum, 1959.
17. AVCO Research Laboratory. Research Reports 1, 3, and 7, by J. A. Fay, F. R. Riddell, P. H. Rose, and W. I. Stark. New York, N.Y., ARL, 1958.
18. Polytechnic Institute of Brooklyn, Department of Aeronautical Engineering and Applied Mechanics. Experimental Temperature Distribution in a Hemispherical Nose Cone in Hypersonic Flow, by S. V. Nardo and J. L. Boccio. New York, N.Y., PIB, June 1959. (Report No. 494.)
19. Air Force Cambridge Research Center. Instrumentation for Studies of the Exploding Wire Phenomenon, by W. G. Chace, and E. H. Cullington. Boston, Mass., AFCRC, 1957. (ASTIA Document No. A.D. 133842.)
20. Wylie, C. R., Jr. Advanced Engineering Mathematics. New York, McGraw-Hill, 1951. P. 75ff.
21. Mayfield, E. B. PHYS REV, 85, 769 (1952).
22. Mayfield, E. B. PHYS REV, 87, 912 (1952).
23. Van Valkenburg, M. E., and C. D. Hendricks, Jr. J APPL PHYS, 26, 776 (1955).
24. White, W. C. ASTROPHYS J, 121, 271 (1955).
25. Allen, W. A., J. S. Rinehart, and W. C. White. J APPL PHYS, 23, 132 (1952).
26. White, W. C. ASTROPHYS J, 122, 559 (1955).

---

#### ACKNOWLEDGMENT

The author wishes to thank Gerald E. Meloy for his assistance in conducting the exploding wire experiments and William A. Allen for his encouragement and support. Dr. Gilbert J. Plain supervised the research and his support and helpful discussions are appreciated. The author is especially indebted to Prof. Franklin S. Harris, Jr. of the University of Utah who proposed the problem and whose encouragement and advice in solving it were invaluable.

INITIAL DISTRIBUTION

- 8 Chief, Bureau of Naval Weapons
  - DLI-31 (2)
  - R-12 (1)
  - RAAV (1)
  - RR (1)
  - RRRE (2)
  - RT-1 (1)
- 1 Chief of Naval Operations (OP 55)
- 3 Chief of Naval Research
  - Code 104 (1)
  - Code 461 (1)
  - Code 463 (1)
- 1 David W. Taylor Model Basin
- 1 Naval Air Development Center, Johnsville
- 1 Naval Air Force, Atlantic Fleet
- 1 Naval Air Force, Pacific Fleet
- 1 Naval Air Material Center, Philadelphia
- 1 Naval Air Station, North Island
- 1 Naval Air Test Center, Patuxent River
- 1 Naval Ammunition Depot, Crane (Research and Development Department)
- 2 Naval Avionics Facility, Indianapolis (Library)
- 2 Naval Missile Center, Point Mugu (Technical Library)
- 1 Naval Ordnance Laboratory, Corona
- 1 Naval Ordnance Laboratory, White Oak (Library)
- 1 Naval Postgraduate School, Monterey
- 2 Naval Research Laboratory (Code 2021)
- 2 Naval Underwater Ordnance Station, Newport
- 1 Naval Weapons Plant (Code 755)
- 2 Naval Weapons Services Office, Naval Weapons Plant
- 1 Navy Electronics Laboratory, San Diego
- 1 Office of Naval Research Branch Office, Pasadena
- 1 Operational Test and Evaluation Force
- 1 Bureau of Naval Weapons Fleet Readiness Representative, Pacific Naval Air Station, North Island
- 1 Bureau of Naval Weapons Representative, Azusa
- 3 Chief of Ordnance
  - ORDTB (1)
  - ORDTS (1)
  - ORDTU (1)
- 2 Aberdeen Proving Ground
  - Ballistic Research Laboratories (1)
  - Development and Proof Services (1)



# ABSTRACT CARD

<p>U. S. Naval Ordnance Test Station  <u>Radiometric Temperature Measurements of Short Duration Events</u>, by Earle B. Mayfield. China Lake, Calif., NOTS, December 1961. 28 pp. (NAWVEPS Report 7796, NOTS TP 2790), UNCLASSIFIED.</p> <p>ABSTRACT. A four-color spectroscope using the wavelengths 0.546, 0.577, 0.623, and 0.750 microns was used to determine the surface temperatures of electrically exploded wires and aluminum projectiles of velocity 4,500 m/sec. Several values of initial</p> <p>○ (Over)  2 cards, 4 copies</p>	<p>U. S. Naval Ordnance Test Station  <u>Radiometric Temperature Measurements of Short Duration Events</u>, by Earle B. Mayfield. China Lake, Calif., NOTS, December 1961. 28 pp. (NAWVEPS Report 7796, NOTS TP 2790), UNCLASSIFIED.</p> <p>ABSTRACT. A four-color spectroscope using the wavelengths 0.546, 0.577, 0.623, and 0.750 microns was used to determine the surface temperatures of electrically exploded wires and aluminum projectiles of velocity 4,500 m/sec. Several values of initial</p> <p>○ (Over)  2 cards, 4 copies</p>
<p>U. S. Naval Ordnance Test Station  <u>Radiometric Temperature Measurements of Short Duration Events</u>, by Earle B. Mayfield. China Lake, Calif., NOTS, December 1961. 28 pp. (NAWVEPS Report 7796, NOTS TP 2790), UNCLASSIFIED.</p> <p>ABSTRACT. A four-color spectroscope using the wavelengths 0.546, 0.577, 0.623, and 0.750 microns was used to determine the surface temperatures of electrically exploded wires and aluminum projectiles of velocity 4,500 m/sec. Several values of initial</p> <p>○ (Over)  2 cards, 4 copies</p>	<p>U. S. Naval Ordnance Test Station  <u>Radiometric Temperature Measurements of Short Duration Events</u>, by Earle B. Mayfield. China Lake, Calif., NOTS, December 1961. 28 pp. (NAWVEPS Report 7796, NOTS TP 2790), UNCLASSIFIED.</p> <p>ABSTRACT. A four-color spectroscope using the wavelengths 0.546, 0.577, 0.623, and 0.750 microns was used to determine the surface temperatures of electrically exploded wires and aluminum projectiles of velocity 4,500 m/sec. Several values of initial</p> <p>○ (Over)  2 cards, 4 copies</p>

NAWMEPS Report 7796

capacitor energy, pressure, and ambient atmosphere were used with the exploded wires. The projectiles were observed in a normal atmosphere at 710 mm Hg.

The temperatures observed for exploded wires for an initial capacitor energy of 0.8 joule in air at 710 mm Hg were:  $3825 \pm 25^\circ\text{K}$  for aluminum,  $3100 \pm 750^\circ\text{K}$  for copper, and  $3700 \pm 250^\circ\text{K}$  for tungsten. For an aluminum projectile in air at 710 mm Hg at a velocity of 4,500 m/sec, the temperature observed was  $3250 \pm 50^\circ\text{K}$ .

The spectral distribution in all cases was observed to be black body and could be fitted by the

(Contd. on Card 2)

NAWMEPS Report 7796

capacitor energy, pressure, and ambient atmosphere were used with the exploded wires. The projectiles were observed in a normal atmosphere at 710 mm Hg.

The temperatures observed for exploded wires for an initial capacitor energy of 0.8 joule in air at 710 mm Hg were:  $3825 \pm 25^\circ\text{K}$  for aluminum,  $3100 \pm 750^\circ\text{K}$  for copper, and  $3700 \pm 250^\circ\text{K}$  for tungsten. For an aluminum projectile in air at 710 mm Hg at a velocity of 4,500 m/sec, the temperature observed was  $3250 \pm 50^\circ\text{K}$ .

The spectral distribution in all cases was observed to be black body and could be fitted by the

(Contd. on Card 2)

NAWMEPS Report 7796

capacitor energy, pressure, and ambient atmosphere were used with the exploded wires. The projectiles were observed in a normal atmosphere at 710 mm Hg.

The temperatures observed for exploded wires for an initial capacitor energy of 0.8 joule in air at 710 mm Hg were:  $3825 \pm 25^\circ\text{K}$  for aluminum,  $3100 \pm 750^\circ\text{K}$  for copper, and  $3700 \pm 250^\circ\text{K}$  for tungsten. For an aluminum projectile in air at 710 mm Hg at a velocity of 4,500 m/sec, the temperature observed was  $3250 \pm 50^\circ\text{K}$ .

The spectral distribution in all cases was observed to be black body and could be fitted by the

(Contd. on Card 2)

NAWMEPS Report 7796

capacitor energy, pressure, and ambient atmosphere were used with the exploded wires. The projectiles were observed in a normal atmosphere at 710 mm Hg.

The temperatures observed for exploded wires for an initial capacitor energy of 0.8 joule in air at 710 mm Hg were:  $3825 \pm 25^\circ\text{K}$  for aluminum,  $3100 \pm 750^\circ\text{K}$  for copper, and  $3700 \pm 250^\circ\text{K}$  for tungsten. For an aluminum projectile in air at 710 mm Hg at a velocity of 4,500 m/sec, the temperature observed was  $3250 \pm 50^\circ\text{K}$ .

The spectral distribution in all cases was observed to be black body and could be fitted by the

(Contd. on Card 2)

# ABSTRACT CARD

<p>U. S. Naval Ordnance Test Station Radiometric Temperature . . . (Card 2) Wien radiation law. Calibration was achieved using a tungsten ribbon lamp.</p> <p>Black-body radiation data from the Planck radiation law are also given using the new value for the second radiation constant, <math>C_2 = 14,388 \mu\text{-}^\circ\text{K}</math> for temperatures from 2000 to 4000°K and wavelengths from 0.500 to 0.800 micron.</p>	<p>○</p> <p>NAVWEPS Report 7796</p>
<p>U. S. Naval Ordnance Test Station Radiometric Temperature . . . (Card 2) Wien radiation law. Calibration was achieved using a tungsten ribbon lamp.</p> <p>Black-body radiation data from the Planck radiation law are also given using the new value for the second radiation constant, <math>C_2 = 14,388 \mu\text{-}^\circ\text{K}</math> for temperatures from 2000 to 4000°K and wavelengths from 0.500 to 0.800 micron.</p>	<p>○</p> <p>NAVWEPS Report 7796</p>
<p>U. S. Naval Ordnance Test Station Radiometric Temperature . . . (Card 2) Wien radiation law. Calibration was achieved using a tungsten ribbon lamp.</p> <p>Black-body radiation data from the Planck radiation law are also given using the new value for the second radiation constant, <math>C_2 = 14,388 \mu\text{-}^\circ\text{K}</math> for temperatures from 2000 to 4000°K and wavelengths from 0.500 to 0.800 micron.</p>	<p>○</p> <p>NAVWEPS Report 7796</p>
<p>U. S. Naval Ordnance Test Station Radiometric Temperature . . . (Card 2) Wien radiation law. Calibration was achieved using a tungsten ribbon lamp.</p> <p>Black-body radiation data from the Planck radiation law are also given using the new value for the second radiation constant, <math>C_2 = 14,388 \mu\text{-}^\circ\text{K}</math> for temperatures from 2000 to 4000°K and wavelengths from 0.500 to 0.800 micron.</p>	<p>○</p> <p>NAVWEPS Report 7796</p>

- 6 Army Rocket and Guided Missile Agency, Redstone Arsenal
  - ORDDW-IDE (1)
  - Rocket Development Laboratory, Test and Evaluation Branch (1)
  - Technical Library, ORDXR-OTL (4)
- 1 Diamond Ordnance Fuze Laboratories
- 2 Frankford Arsenal
  - Pitman Dunn Laboratory (1)
  - Library (1)
- 2 Picatinny Arsenal (Library)
- 1 Rock Island Arsenal
- 1 Watertown Arsenal
- 3 White Sands Proving Ground
- 2 Headquarters, U. S. Air Force
  - 1 Aeronautical Systems Division, Wright Patterson Air Force Base (ASAPRD-Dist)
  - 1 Air Force Cambridge Research Laboratories, Laurance G. Hanscom Field
  - 1 Air Force Special Weapons Center, Kirtland Air Force Base
  - 1 Air Proving Ground Center, Eglin Air Force Base
  - 1 Holloman Air Force Base
  - 1 Tactical Air Command, Langley Air Force Base (TPL-RQD-M)
  - 1 Air Force Development Field representative, Aberdeen Proving Ground
- 10 Armed Services Technical Information Agency (TIPCR)
  - 1 Defense Atomic Support Agency, Sandia Base (Development Division)
  - 1 Ames Research Center
  - 1 Langley Research Center (Library)
  - 1 Lewis Research Center
  - 1 AeroChem Research Laboratories, Inc., Princeton, N. J.
  - 1 Aerojet-General Corporation, Azusa, Calif., via BuWepsRep
  - 2 Aerospace Corporation, Los Angeles
    - Dr. Earle Mayfield (1)
    - Library (1)
  - 2 Applied Physics Laboratory, JHU, Silver Spring
  - 1 Armour Research Foundation, Chicago (G. A. Nothmann)
  - 1 Arthur D. Little, Inc., Cambridge
  - 1 AVCO Research Laboratory, Everett, Mass. (Document Control Center)
  - 1 Boeing Airplane Company, Seattle (Branch 7 Library)
  - 1 General Electric Advanced Electronics Center, Ithaca (Librarian)
  - 1 Hughes Aircraft Company, Culver City, Calif. (Research and Development Library)
  - 1 Jet Propulsion Laboratory, CIT, Pasadena (Dr. W. H. Pickering)
  - 1 Rohm and Haas Company, Redstone Arsenal Research Division (Librarian)
  - 1 The Rand Corporation, Santa Monica, Calif.
  - 1 Thiokol Chemical Corporation, Redstone Division, Redstone Arsenal, (Technical Library)
  - 1 University of Maryland, Department of Physics, College Park